Tumor Biol. (2016) 37:11843–11859
DOI 10.1007/s13277-016-5041-y

ORIGINAL ARTICLE

Evidence for embryonic stem-like signature and epithelial-mesenchymal transition features in the spheroid cells derived from lung adenocarcinoma

Raheleh Roudi[1,2,3] · Zahra Madjd[1,2,3] · Marzieh Ebrahimi[4] · Ali Najafi[5] · Alireza Korourian[2] · Ahmad Shariftabrizi[6] · Ali Samadikuchaksaraei[3]

Received: 16 November 2015 / Accepted: 28 March 2016 / Published online: 5 April 2016

Abstract Identification of the cellular and molecular aspects of lung cancer stem cells (LCSCs) that are suggested to be the main culprit of tumor initiation, maintenance, drug resistance, and relapse is a prerequisite for targeted therapy of lung cancer. In the current study, LCSCs subpopulation of A549 cells was enriched, and after characterization of the spheroid cells, complementary DNA (cDNA) microarray analysis was applied to identify differentially expressed genes (DEGs) between the spheroid and parental cells. Microarray results were validated using quantitative real-time reverse transcription-PCR (qRT-PCR), flow cytometry, and western blotting. Our results showed that spheroid cells had higher clonogenic potential, up-regulation of stemness gene Sox2, loss of CD44 expression, and gain of CD24 expression compared to parental cells. Among a total of 160 genes that were differentially expressed between the spheroid cells and the parental cells, 104 genes were up-regulated and 56 genes were down-regulated. Analysis of cDNA microarray revealed an embryonic stem cell-like signature and over-expression of epithelial-mesenchymal transition (EMT)-associated genes in the spheroid cells. cDNA microarray results were validated at the gene expression level using qRT-PCR, and further validation was performed at the protein level by flow cytometry and western blotting. The embryonic stem cell-like signature in the spheroid cells supports two important notions: maintenance of CSCs phenotype by dedifferentiating mechanisms activated through oncogenic pathways and the origination of CSCs from embryonic stem cells (ESCs). PI3/AKT3, as the most common up-regulated pathway, and other pathways related to aggressive tumor behavior and EMT process can confer to the spheroid cells' high potential for metastasis and distant seeding.

Keywords Cancer stem cells · Lung cancer · cDNA microarray · Sphere formation assay · Embryonic stem cell-like signature

Electronic supplementary material The online version of this article (doi:10.1007/s13277-016-5041-y) contains supplementary material, which is available to authorized users.

✉ Zahra Madjd
Zahra.madjd@yahoo.com; Madjd.z@iums.ac.ir

✉ Marzieh Ebrahimi
Mebrahimi@royaninstitute.org

[1] Oncopathology Research Center, Iran University of Medical Sciences, Tehran, Iran

[2] Department of Molecular Medicine, Faculty of Advanced Technologies in Medicine, Iran University of Medical Sciences, Tehran, Iran

[3] Cellular and Molecular Research Center, Iran University of Medical Sciences, Tehran, Iran

[4] Department of Stem Cells and Developmental Biology at Cell Science Research Center, Royan Institute for Stem Cell Biology and Technology, ACECR, Tehran, Iran

[5] Molecular Biology Research Center, Baqiyatallah University of Medical Sciences, Tehran, Iran

[6] Department of Nuclear Medicine and Molecular Imaging, State University of New York at Buffalo, Buffalo, NY 14214, USA

Introduction

Lung cancer is the most common cancer and the leading cause of cancer-related death throughout the world [1, 2]. The high aggressiveness and devastating nature of a variety of tumor types, including lung cancer, is attributed to the presence of a subpopulation of extremely high tumorigenic cancer cells termed cancer stem cells (CSCs) or cancer initiating cells (CICs) [3]. These hyper-malignant cancer cells have the ability to initiate and maintain tumor growth, confer resistance to conventional radio/chemotherapy regimens, and promote recurrence and metastasis [4, 5]. Detailed knowledge concerning the genomic profiles of CSCs is required to determine the genetic changes associated with initiation, progression, and metastasis of lung cancer. To our knowledge, limited data is available addressing the gene expression profiling of lung CSCs [6, 7].

Since CSCs possess common basic characteristics and signal transduction pathways with normal stem cells, isolation and characterization of CSCs can be accomplished by using their phenotypic similarities, including expression of cell surface markers, sphere-forming assays, and dye exclusion [5, 8]. Numerous efforts have been directed to characterize lung CSCs using putative CSC cell surface markers including CD133 and CD44, the intracytoplasmic enzyme activity of aldehyde dehydrogenase 1 (ALDH1) and the efflux of Hoechst 33342 by the ATP-binding cassette (ABC) family [7, 9–18]. Despite applying different approaches, no definite lung CSC marker(s) has been identified for isolation of CSCs in lung cancer; therefore, further attempts are required to explore CSCs subpopulation(s) in lung cancer. The ability of undifferentiated stem cells to form free-floating clusters under non-adherent conditions, known as spheres, have been widely used in recent years as an approach for the enrichment of CSCs in several malignancies including lung cancer [19–22].

Our previous flow cytometric analysis of a panel of putative stem cell markers in human lung adenocarcinoma epithelial cell line, A549, did not show any specific CSC marker for this cell line [23]. The self-renewal ability of stem cell allows for forming as free-floating structures called sphere in suspension culture in medium not containing serum, and this approach was widely used for identification of CSCs from various tissues and malignant tumors [21]. Therefore, in the present study, enrichment of CSCs was performed by plating A549 cells in non-adherent and serum-free conditions. Then, the spheroid cells were characterized using the colony-formation assay, quantitative real-time reverse transcription-PCR (qRT-PCR) for evaluating stemness-related genes and flow cytometry for determining putative stem cell markers. In the next phase, gene expression profiling of the spheroid cells compared to the parental cells was analyzed using complementary DNA (cDNA) microarray to identify differentially expressed genes (DEGs), distinctive signal transduction pathways, and gene expression signatures. Since our gene expression analysis showed significant over-expression of c-KIT in the spheroid cells, the expression levels of c-KIT protein was determined by immunohistochemical analysis on tissue microarray (TMA) samples of different subtypes of lung cancer.

Materials and methods

Cell culture and sphere formation

The human lung adenocarcinoma epithelial cell line A549 was obtained from the Iranian Biological Resource Center (IBRC C10080, Tehran, Iran) and maintained as monolayer culture in Dulbecco's modified Eagle's medium (DMEM; Gibco, Invitrogen, USA), 10 % fetal calf serum (FCS; Gibco, Invitrogen, USA), 2 mM L-glutamine, 2 mM non-essential amino acid, 100 U/ml penicillin, and 100 μg/ml streptomycin known as a complete medium at 37 °C in a humidified atmosphere containing 5 % CO_2.

To form the spheroids, the poly-hydroxyethyl methacrylate (poly-HEMA) (Sigma, USA) coating was used to prevent cell adhesion. A stock solution of poly-HEMA was prepared by dissolving 1.2 g of poly-HEMA in 10 ml of 95 % ethanol, then diluted 1:10 to obtain the final solution at 1.2 % and filtered. Tissue culture flasks were coated with the diluted solution and allowed to air-dry in a laminar flow hood overnight. Approximately 7×10^5 of single viable cells were plated on poly-HEMA coated tissue culture flasks in serum-free media as described previously [23]. For passage of spheres with the mean size of 250–300 μm, the collected free-floating spheres were washed with PBS, then dissociated by treatment with trypsin-EDTA and gentle pipetting, re-suspended in serum-free media to re-form spheres and were passaged every 4–6 days. In the current study, all comparisons were made between the third passage sphere-forming cells (termed spheroid cells) and parental A549 cells (termed parental cells).

Colony-formation assay

For the colony-formation assay, single cell mixture of parental cells and spheroid cells were prepared, then an equal cell number of each population was seeded at a density of 80 viable single cells/well on six-well culture plates in complete medium and allowed to grow for 10 days. The cell colonies were fixed with 4 % paraformaldehyde and stained with 0.05 % crystal violet (Sigma, USA). Colonies with more than 50 cells were counted and colony-forming efficiency was determined by the method described previously [23]. Moreover, the number of different colony types (holoclone, meroclone, and paraclone) was determined in each population. Large colonies with small compact cells, homogeneous cell morphology, and regular margins were

identified as holoclone, whereas paraclones were fragmented assemblies of fully differentiated cells with irregular margins and aborted cells. The third colony type known as meroclones harbored heterogeneous cell populations, were medium-sized, and showed the intermediate structure between holoclones and paraclones.

Total RNA extraction, cDNA synthesis, and qRT-PCR

Total RNA from parental cells and the spheroid cells were extracted by the Trizol method (Sigma, USA) according to the manufacturer's standard procedures. For complete DNA digestion, total RNA was treated with RNase-free DNase I (Fermentas, Germany), and its purity and integrity were determined by spectrophotometry and agarose gel electrophoresis, before and after treatment. cDNA was synthesized from 2 μg DNase I-treated total RNA using RevertAidTM first Strand cDNA Synthesis Kit (Fermentas, Germany). Expression of common stemness genes including c-Myc, Klf4, Sox2, Oct4, and Nanog was examined by applying qRT-PCR. For each PCR, 2 μl of diluted template cDNA (16 ng/μl) was quantified using 10 μl of SYBR®Premix Ex Taq™ II (RR081Q, Takara Bio., Inc.), 6 μl dH_2O, and 1 μl each of the forward and reverse primers (5 pmol/μl) in a Rotor-Gene™ 6000 Real-Time PCR System (Corbett Life Science, Sydney, Australia) using the following program: 95 °C for 10 min (stage 1) and 95 °C for 10 s, 60 °C for 20 s, and 72 °C for 20 s (stage 2), for 40 cycles. Average expression of GAPDH gene was used to normalize expression values. All data are represented as log2-linear plots. The sequence-specific primers are shown in Table 1.

Immunophenotyping of promising CSC markers

The protein expression of some putative CSC markers including CD24, CD133, ABCG2, and CD44/CD24 were analyzed in the spheroid cells and compared to parental cells using flow cytometry. For this purpose, single cell suspensions from each population were prepared by the method described above, and then at least 1×10^5 cells of each population were incubated with 1 mg/ml of fluorescently labeled monoclonal antibodies or respective isotype controls at 4–8 °C for 30 min on ice at dark. After washing, labeled cells were analyzed by flow cytometry using fluorescence-activated cell sorting (FACS) Aria II (Becton Dickinson, San Jose, CA, USA). The following antibodies were used for flow cytometry: phycoerythrin (PE)-labeled mouse anti-human CD133, PE-labeled mouse anti-human CD44, PE-labeled mouse anti-human ABCG2, and fluorescein isothiocyanate (FITC)-labeled mouse anti-human CD24 (all from Dako). All data were analyzed using CellQuest software (Becton Dickinson, San Jose, CA, USA).

RNA and cDNA preparation for cDNA microarray

Total RNA was extracted from parental cells and spheroid cells using an RNeasy Mini Kit (Qiagen, USA) according to the manufacturer's protocol. Briefly, cell pellets were lysed, homogenized by RLT buffer (Qiagen), and loaded onto an RNeasy spin column and centrifuged. Then RW1 buffer (Qiagen) was added and centrifuged, the remaining contamination was washed by adding modified PRE buffer (Qiagen), and the RNA was diluted. In total RNA extraction, RPE buffer was used for elimination of proteins and salts such as guanidine salt. In Qiagen kit (cat number: 74104), buffer RPE is supplied as a concentrate. Before using for the first time, four volumes of ethanol (96–100 %) were added to obtain a working solution.

After evaluation of concentration, purity, and quality of samples, 50 μg of total RNA from each population were reversed transcribed using the Amino Allyl cDNA labeling kit (Ambion, USA) according to the manufacturer's instructions. In the first step, cDNA was constructed from total RNA by reverse transcription: dTTP was partially substituted with aminoallyl dUTP, the RNA was removed from the cDNA,

Table 1 Sequence-specific primers of targeted stemness genes used for qRT-PCR

Primer	Sequence (5′→3′)	Product size (bp)	Ta (°C)
GAPDH	F: CTCATTTCCTGGTATGACAACGA	122	60
	R: CTTCCTCTTGTGCTCTTGCT		
c-Myc	F: ACACATCAGCACAACTACG	140	60
	R: CGCCTCTTGACATTCTCC		
Klf4	F: ATTACCAAGAGCTCATGCCA	150	60
	R: CCTTGAGATGGGAACTCTTTG		
Sox2	F: GGGAAATGGAAGGGGTGCAAAAGAGG	151	60
	R: TTGCGTGAGTGTGGATGGGATTGGTG		
Nanog	F: AAAGAATCTTCACCTATGCC	110	60
	R: GAAGGAAGAGGAGAGACAGT		
Oct4	F: CTGGGTTGATCCTCGGACCT	128	60
	R: CACAGAACTCATACGGCGGG		

and the amino allyl-modified cDNA was recovered by ethanol precipitation. In the second step, the amino allyl-modified cDNA was coupled to the fluorescent dye by incubation of the cDNA with either Cy3 or Cy5 (Amersham Biosciences, Buckinghamshire, UK), terminated by addition of hydroxylamine, passed through a Nuc-Away Spin Column to remove the free dye, and the end cDNA concentration and Cy5/Cy3 incorporation were evaluated.

Microarray hybridization, scanning, and data processing

The Ocimum Biosolutions Human Cancer OciChip ™ (Ocimum Biosolutions, India) array was used for comparison of gene expression profiles of the spheroid cells and parental cells. This array covers 1853 human genes associated with cancer progression and spans genes associated with a wide range of biological pathways including cell cycle control, cell adhesion, angiogenesis, signaling, and immunity. An equal amount of each labeled cDNA target was fragmented with a hybridization buffer (BioTray, Lyon, France) at 94 °C for 5 min using a thermal cycler (Eppendorf, Germany). Hybridization and washing were performed using the automated system Tray Mix S4 (BioTray, Lyon, France) based on the chaotic hybridization approach. After hybridization and washing, the slides were dried and scanned immediately with a two-channel cDNA microarray system, ScanArray Express HT scanner (PerkinElmer, Waltham, MA, USA). The scanner software recognizes the regions of fluorescent signal, determines the signal intensity, and compiles the data into a spreadsheet of fluorescent signals of every probe on the array. The Lowess normalization method was used to normalize the Cy5:Cy3 intensity ratios for each data point [24]. This process was carried out for three different biological replicate of spheroid and parental cells, respectively, to increase the accuracy. Further analysis of the DEGs selection was performed using GPRocessor 2.0, a software developed at Yale University (New Haven, CT, USA).

Functional gene analysis, construction of PPI network and signaling pathway mapping

For functional gene expression analysis, DEGs were submitted to the Visualization and Integrated Discovery (DAVID) web-based tool (http://david.abcc.ncifcrf.gov/), while for Gene Ontology (GO) terms, enrichment analysis was applied ($P < 0.05$). The applied threshold was adopted from fisher exact P value for gene enrichment analysis where $P < 0.05$ represents significant enrichment. Also, construction of the protein-protein interaction (PPI) network between DEGs was performed using the STRING web-based tool (http://string-db.org) [25]. In reconstructing the pertinent PPI networks, only interactions with a probabilistic confidence score of at least 0.4 were selected. Network parameters were analyzed using a Network Analyzer of Cytoscape (http://www.cytoscape.org/) for the spheroid cells' PPI network. A P value of ≤ 0.05 was considered to be statistically significant.

To identify the spheroid-specific signaling pathways, all 160 DEGs discovered by the microarray were mapped into Kyoto Encyclopedia of Genes and Genomes (KEGG), REACTOME, BIOCARTA, and other signaling pathway databases [26–28] (the full list of pathway databases can be found in the Path Guide website, www.pathguide.org). Based on these signaling pathway databases, and previous literature, the spheroid-specific signaling pathways were manually constructed using CellDesigner version 4.4 (www.celldesigner.org) in Systems Biology Markup Language (SBML) format, which provides the capabilities of graphical environment, pathway visualization, and navigation.

Validation of cDNA microarray results at the gene level by qRT-PCR analysis

For validation of cDNA microarray results by qRT-PCR, 15 genes were selected from the DEGs list based on their putative role in tumor progression and metastasis, epithelial-mesenchymal transition (EMT), embryonic signaling pathways, and putative stem cell markers (Table 2). Sequence-specific primers were designed with the aid of the primer3 web tool (http://biotools.umassmed.edu/bioapps/primer3_www.cgi) against the coated nucleotide sequences on the array slide (Table 3). After determination of the specificity of each primer set and the molecular weight of the amplicon, qRT-PCR was performed on a Rotor-Gene™ 6000 Real-Time PCR System according to the above-mentioned methods. Specific amplification was confirmed using negative controls and dissociation curves.

Further validation of cDNA microarray results at the protein level by flow cytometry and western blot

The protein expression of chemokine (C-X-C motif) ligand 12 (CXCL12) also called stromal cell-derived factor 1 (SDF1), as the most up-regulated transcript in our spheroid cells, was assessed by western blot. For each cell population (spheroid and parental cells), 30 μg proteins were separated by 10 % SDS-PAGE gel electrophoresis at 100 V for 2 h using a Mini-PROTEAN 3 electrophoresis system (Bio-Rad, Hercules, CA, USA) and transferred to a PVDF membrane (Amersham) using a semi-dry blotting method (Bio-Rad) and Dunn carbonate transfer buffer (10 mM NaCHO3, 3 mM Na2CO3, 20 % methanol). After washing, each membrane was blocked with blocking buffer (5 % nonfat dry milk in TBS-tween-20 (0.05 %)) for 1.5 h at room temperature (RT) with gentle agitation. The membranes were incubated with primary antibodies against CXCL12 or

Table 2 Fifteen genes from different pathways were selected for validation by qRT-PCR

Function	Gene selected from DEGs
Tumor progression and metastasis	CXCL12, CDH6, c-KIT, CD24, PDGFRA
Epithelial-mesenchymal transition (EMT)	BMPR1B, FZD4, SMO, c-KIT, WNT10B, CDH6
Embryo lung development and embryonic signaling pathways	SMO, NOTCH2, WNT10B, BMPR1B, FZD4, c-KIT
Cell cycle G1/S phase transition	CDK2
Regulation of programmed cell death	BAD
Angiogenesis	PDGFRA, SIRT1
Stem cell markers	CD24, c-KIT
Components of the extracellular matrix	HAS1
Cell proliferation and tumor growth	PTH1R, c-KIT

SDF1) (Cell Signaling, 3740, 1:1000) and GAPDH (1:20000 as the housekeeping gene or internal control) for 2 h at RT with gentle agitation. At the end of the incubation period, the membranes were washed and incubated with the peroxidase-conjugated secondary antibody (anti-rabbit (Millipore, Billerica, MA, USA, 1:300000)) for 1 h at RT with gentle agitation. Eventually, visualization was performed using an ECL advance western blotting detection kit (GE Healthcare, USA), and X-ray films (Agfa, Mortsel, Belgium) were scanned with a densitometer (GS-800, Bio-Rad, USA). In addition, the analysis of CD24 protein expression in

Table 3 Sequence-specific primers of 15 selected genes for the validation of microarray data using qRT-PCR

Primer	Sequence (5′ → 3′)	Product size (bp)	Ta (° C)
CXCL12	F: AAGAACAACAACAGACAAGTG	109	60
	R: GCAACATGGCTTTCGAAGA		
CDK2	F: TTGTCAAGCTGCTGGATGTC	112	60
	R: TGGAGCAGCTGGAACAGATA		
PTH1R	F: CACCTGTTCCTGTCCTTCAT	234	60
	R: CTCCACCAGAATCCAGTAGTAG		
BMPR1B	F: CAAAGGTCTTGCGTTGTAAATG	150	60
	R: AGCCTTCTAGTCCTAGGCAACC		
FZD4	F: GGGTCAGTTACCAGTGACCTTC	151	60
	R: CGTCCCCATCCTAGATCAGTTA		
CD24	F: TCCTACCCACGCAGATTTATTC	154	60
	R: ACGAAGAGACTGGCTGTTGACT		
c-KIT	F: CGAGTTGGCCCTAGACTTAGAA	140	60
	R: TTGTGATCCGACCATGAGTAAG		
PDGFRA	F: TTGGTGAGAGTCCAACAGACAC	152	60
	R: AGGGAAGTACATGGATGGATTG		
HAS1	F: GATACTGGGTAGCCTTCAATGTG	128	60
	R: GTTGTACCAGGCCTCAAGAAACT		
SMO	F: TATTCCTCTCCCAGGTGTTTGT	147	60
	R: ACCGCTGAAACTGAACTGAAAT		
BAD	F: CGAGTCTTCCAGTCCTGGTG	137	60
	R: GTACTTCCGCCCATATTCAAGA		
SIRT1	F: TATTTATGCTCGCCTTGCTGTA	145	60
	R: ACAGAGAGATGGCTGGAATTGT		
NOTCH2	F: ACCTATCTGCATGGACCTCTGT	151	60
	R: CAATTTGGTCTGACATTGTGCT		
WNT10B	F: TGGTCCCTGGAAGCTTAAAGTA	145	60
	R: GGTGTCTAAGGAGCAGAAGAGG		
CDH6	F: GTCGGTACATTTGTTGTCCAAGT	151	60
	R: TGTTGAGCAAAGCTGTCTTGATA		

spheroid cells compared to parental cells was performed as described in the above section (Immunophenotyping of promising CSC markers).

Immunohistochemistry of c-KIT

The expression levels of c-KIT protein were examined on a series of lung TMA, including 51 squamous cell carcinoma (SCC), 37 adenocarcinoma (ADC), and 8 large cell carcinoma (LCC) as non-small cell lung cancer (NSCLC), and 26 small cell lung cancer (SCLC). Immunohistochemistry was performed using rabbit polyclonal anti-c-KIT antibody (Santa Cruz, USA, dilution 1:50) as described previously [29, 30]. The immunostained TMA slides were evaluated by two observers (A.K. and Z.M.) and scored based on the intensity of staining, percentage of positive cells, and histochemical score (*H*-score). The latter was assigned by multiplying the staining intensity by the percentage of positive tumor cells [31].

Statistical analysis

The data concerning the in vitro characterization of spheroid cells are presented as mean ± SD obtained from at least three different experiments. Student's *t* test was performed to evaluate the difference between the mean values. The correlation between c-KIT expression of (as detected by immunohistochemistry) and lung tumor types was evaluated using Pearson's χ^2 and Pearson's *R* tests. Moreover, the expression level of c-KIT in various subtypes of NSCLC (including SCC, ADC, and LCC) were compared using Mann-Whitney *U* test.

Results

Spheroids cells derived from parental cells were clonogenic and expressed higher levels of Sox2 mRNA

Spheroids from parental cells formed free-floating cellular aggregates and were in a very compact spherical shape (Fig. 1a–c). The spheroid cells were serially passaged using a similar procedure and propagated as pulmospheres for nine passages, but the number and mean size of the spheroids reduced by serial passage. To explore the cancer stem cell-like properties of spheroids cells, their colony-forming potential was compared with parental cells. The spheroid cells, similar to parental cells, were able to form three kinds of colonies with different characteristics including holoclone, meroclone, and paraclone (Fig. 1d). The spheroid cells formed significantly more holoclones ($P = 0.003$) and paraclones ($P < 0.001$) than the parental cells (Fig. 1e). The parental cells displayed colony-forming potential of 56.66 ± 0.72 % with mean colony size of 2919 ± 146 μm, whereas colony-forming potential for spheroid cells was 67.08 ± 0.72 % with mean colony size of 5549 ± 277 μm. Therefore, the spheroid cells showed significantly higher clonogenic capacity ($P < 0.001$) (Fig. 1e) and larger colonies ($P = 0.009$) (Fig. 1f) than parental cells. For further characterization of spheroids, expression of stemness-related genes c-Myc, Nanog, Klf4, Oct4, and Sox2 in the spheroid cells were compared with the parental cells. The spheroid cells expressed higher levels of Sox2 ($P = 0.038$) and Oct4 ($P > 0.05$) and lower levels of c-Myc ($P = 0.04$) and Nanog ($P > 0.05$) genes. There was no significant difference in the expression of Klf4 gene between the two populations (Fig. 1g).

Loss of CD44 expression and gain of CD24 expression in spheroid cells

Flow cytometric analysis of putative stem cell markers CD44/CD24 demonstrated that parental cells expressed $CD44^+/CD24^+$ at mean level of 64.1 ± 2.02 %, whereas the mean level of $CD44^+/CD24^+$ expression in the spheroid cells was 51.02 ± 0.9 % (Table 4). Furthermore, the mean expression of $CD44^+/CD24^{-/low}$ population was 27.92 ± 3.63 % and 15.47 ± 1 % in parental cells and spheroid cells, respectively (Table 4). These findings revealed that the $CD44^+/CD24^+$ and $CD44^+/CD24^{-/low}$ populations were significantly smaller in the spheroid cells compared to the parental cells ($P = 0.002$ and $P = 0.02$, respectively). Our results showed that $CD44^-/CD24^+$ cells were not frequently found in parental cells (mean ± SD; 0.2 ± 0.3 %), whereas $CD44^-/CD24^+$ was expressed in 13.73 ± 0.7 % of spheroid cells (Table 4). Moreover, $CD44^-/CD24^{-/low}$ cells constituted less than 2 % of parental cells (mean ± SD; 1.68 ± 0.69 %), but 19.78 ± 0.4 % of spheroid cells expressed $CD44^-/CD24^{-/low}$ (Table 4). These findings suggest that the $CD44^-/CD24^+$ and $CD44^-/CD24^{-/low}$ populations were significantly higher in the spheroid cells compared to parental cells ($P = 0.0002$ and $P < 0.0001$, respectively). Also, the evaluation of promising stem cell markers CD133 and ABCG2 by flow cytometry showed no significant difference between the spheroid and parental cells ($P > 0.05$).

Spheroid cells derived from parental cells displayed embryonic stem cell-like gene expression signature

Comparison of the gene expression pattern of spheroid cells with parental cells (with cutoff signal log ratio ≥1 or ≤−1 [24])

Fig. 1 Characterization of the spheroids derived from A549 lung adenocarcinoma cells. **a**–**c** The spheroid cells were free-floating clusters of compacted cells. **d** Three colony types named as holoclone, meroclone and paraclone were identified during the colony-formation assay in both parental and spheroid cells. **e** The potential of clonogenicity and **f** the size of colonies were significantly higher in the spheroid cells. **g** Evaluation of stemness-related genes using qRT-PCR. Spheroid cells had significantly higher expression level of Sox2 and lower expression level of c-Myc. Data is presented as mean ± SD of at least three different experiments

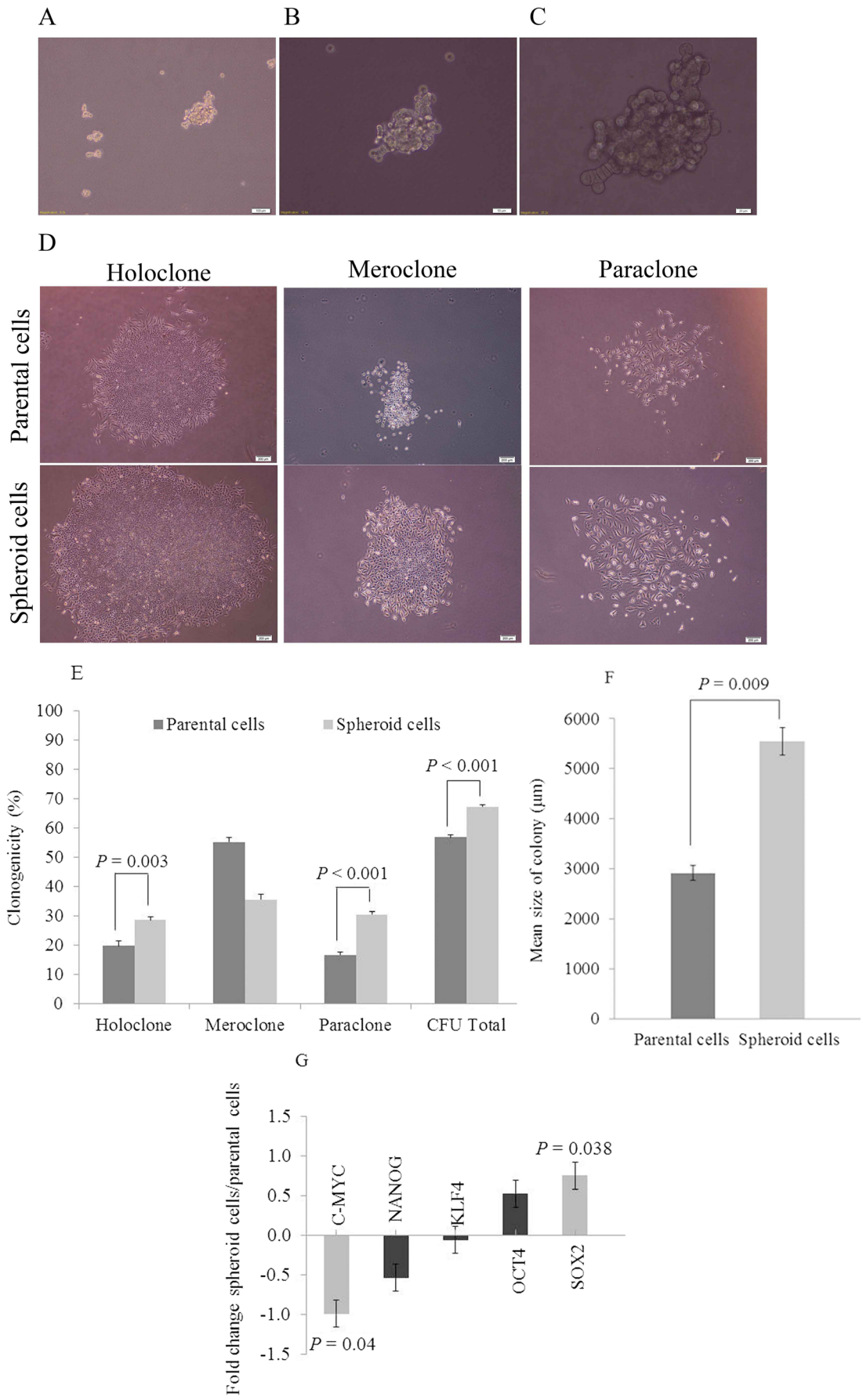
A
B
C
D
Holoclone
Meroclone
Paraclone
Parental cells
Spheroid cells
E
Parental cells
Spheroid cells
Clonogenicity (%)
P = 0.003
P < 0.001
P < 0.001
Holoclone
Meroclone
Paraclone
CFU Total
F
P = 0.009
Mean size of colony (µm)
Parental cells
Spheroid cells
G
Fold change spheroid cells/parental cells
C-MYC
NANOG
KLF4
OCT4
SOX2
P = 0.04
P = 0.038

Table 4 Flow cytometric analysis of putative stem cell markers CD44/CD24, CD133, and ABCG2 in the spheroid cells compared to parental cells

Putative marker	Mean percentage of positive cells ± SD	
	Spheroid cells (%)	Parental cells (%)
$CD44^+/CD24^+$	51.2 ± 0.9	64.1 ± 2.02
$CD44^+/CD24^{-/low}$	15.47 ± 1	27.92 ± 3.63
$CD44^-/CD24^+$	13.73 ± 0.7	0.2 ± 0.3
$CD44^-/CD24^{-/low}$	19.78 ± 0.4	1.68 ± 0.69
CD133	0.36 ± 0.07	0.94 ± 0.05
ABCG2	0.15 ± 0.02	0.91 ± 0.05

revealed that 160 transcripts were differentially expressed: 104 genes were up-regulated and 56 were down-regulated. A complete list of DEGs is provided as supplementary file 1. Official symbols were used according to the genes' IDs and lists were approved by the Human Gene Nomenclature Committee (HGNC) (http://www.gene.ucl.ac.uk/nomenclature/)[32].

The DEGs were functionally categorized using the Visualization and Integrated Discovery (DAVID) web-based tool (http://david.abcc.ncifcrf.gov/); while for Gene Ontology (GO) terms, enrichment analysis was applied ($P < 0.05$) [33]. Thus, DEGs were categorized into 11 groups according to their function, including positive regulation of cell proliferation, positive regulation of macromolecule metabolic process, regulation of apoptosis, regulation of programmed cell death, cell surface receptor linked signal transduction, protein modification processes, cellular protein metabolic processes, regulation of nucleic acid metabolic processes, regulation of gene expression, and regulation of cellular biosynthetic processes (Fig. 2).

Eleven signaling pathways including phosphatidylinositol 3-kinase/AKT (PI3K/AKT), Ras, Rap1, RAS-mitogen activated protein kinase/extracellular signal-regulated kinase (MAPK/ERK), Janus kinases/signal transducers and activators of transcription (JAK/STAT), AMPK, nuclear factor kappa-B (NF-kB), TNF, P53, Hedgehog, and Notch pathways were found to be preferentially expressed in the spheroid cells compared to the parental cells (Table 4). Thirty-two genes (26 were up-regulated and six down-regulated) were mapped by bioinformatics' tools and assigned to these pathways. Some of the genes could be mapped in multiple pathways, including inhibitor of nuclear factor kappa-B kinase subunit gamma (IKBKG) (five signaling pathways), alpha-type platelet-derived growth factor receptor (PDGFRA) (four signaling pathways), and insulin-like growth factor 1 (IGF-1) receptor (IGF1R) and v-kit Hardy-Zuckerman 4 feline sarcoma viral oncogene homologue (c-KIT or CD117) (three signaling pathways) (Fig. 3 and Table 5). The most up-regulated gene in the spheroid cells was chemokine (C-X-C motif) ligand 12 (CXCL12) which plays a critical role in tumor progression and metastasis [34]. Furthermore, a number of genes known to be involved in epithelial-mesenchymal transition (EMT) process, a prerequisite for cancer invasion and metastasis, were detected in the list of DEGs, including cadherin-6 (CDH6), matrix metallopeptidase14 (MMP14), and wingless-type MMTV integration site family, member 10B (WNT10B). Spheroid cells also overexpressed RAB27A (a member of RAS oncogene family), RAB36 (a member of RAS oncogene family), and RAB10 (a member of RAS oncogene family) that promote metastatic behavior in cancer cells. In parallel with the flow cytometry results for characterization of spheroid cells, over-expression of the putative embryonic stem cell marker CD24 was also noted in the DEG analysis.

Construction of the spheroid cells PPI network

In the PPI network of the spheroid cells with 105 nodes and 154 edges, cyclin-dependent kinase 2 (CDK2) was a hub gene with the highest connectivity degree of 14 and after that MRE11A gene is located with connectivity degree of 11

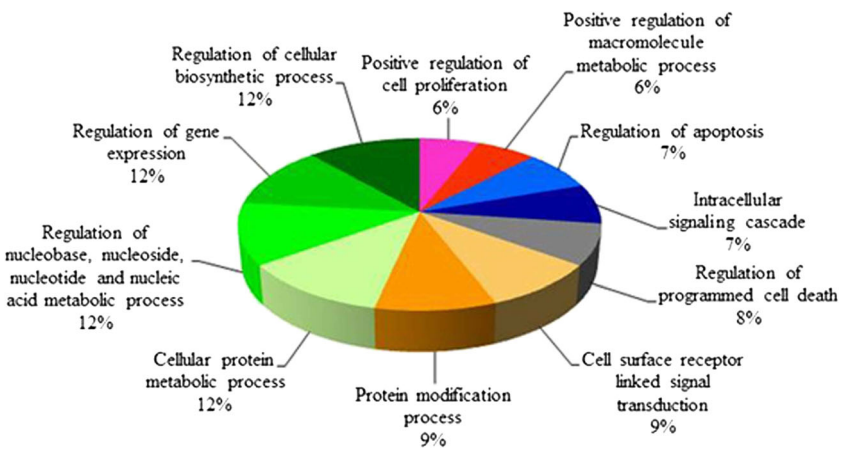

Fig. 2 Differentially expressed genes (DEGs) were categorized into 11 groups according to their function

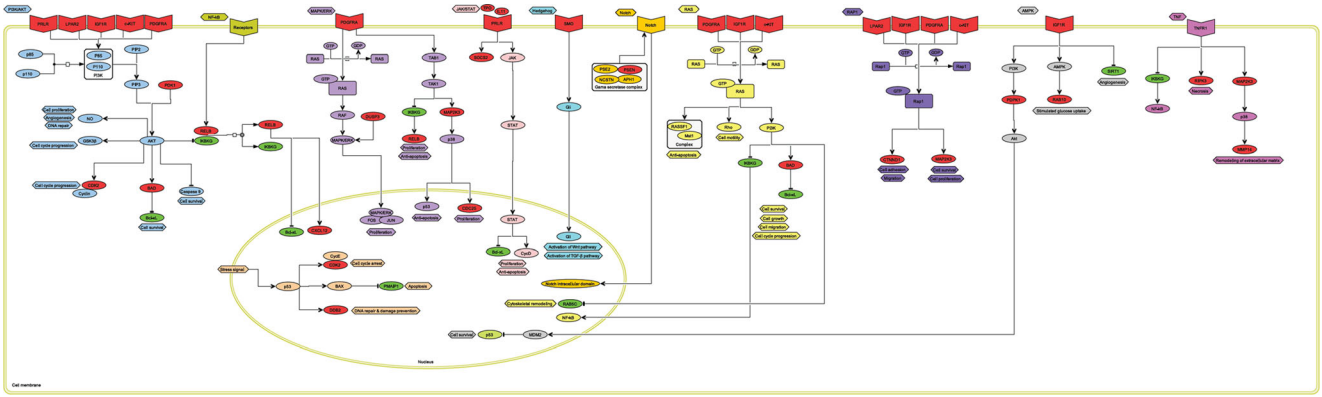

Fig. 3 The differentially expressed pathways between the spheroid cells and parental cells. Component of each pathway is shown with a distinct color, whereas up-regulation and down-regulation of each pathway is depicted with *red* and *green* colors, respectively (from left to the right; PI3/AKT: blue, NF-kB: dark green, MAPK/ERK: purple, JAK/STAT: pale pink, Hedgehog: pale green, Notch: orange, Ras: yellow, Raf1: dark blue, AMPK: gray, TNF: dark pink, P53: pale orange)

(Fig. 4). The order of high to low connectivity degree was BLM, TOP1, SIRT1, WRN, ERCC5, SMARCA4, PSEN1, and BCL6. CDK2, SMARCA4, and BCL6 were components of sub-network-1 and other genes, except for SIRT1, and PSEN1 were interacting in the sub-network 2 (Fig. 4).

cDNA microarray results showed a robust correlation with qRT-PCR analysis

The reproducibility of the microarray data was confirmed by qRT-PCR analysis of a panel of selected genes. Comparison of the spheroid cells with the parental cells demonstrated that changes in gene expression levels were similar to the array data, in 13 out of the 15 studied genes, and there was a robust correlation between microarray data and qRT-PCR gene expression results (86.66 %) (Fig. 5a). All data are presented as log2-linear plots.

Protein levels of CD24 and CXCL12 were increased in spheroid cells

The mean expression level of putative stem cell marker CD24 was 55.3 ± 1 % in parental cells, whereas the spheroid cells expressed CD24 at 68.1 ± 0.7 % mean level. Therefore, CD24 expression was significantly increased in the spheroid cells compared to the parental cells ($P = 0.002$). Furthermore, the increased level of CXCL12 protein expression (a protein involved in tumor progression and metastasis), was confirmed by western blotting. Thus, both CXCL12 protein and transcript were highly overexpressed in the spheroid cells compared with parental cells (Fig. 5b).

Elevated expression of c-KIT in ADC tumors

Since up-regulation of c-KIT gene was observed at DGEs list; we performed immunohistochemical analysis to explore expression c-KIT protein in various lung tumor subtypes. Normal lung tissue was included in each block of tissue array as a normal control for expression of c-KIT. Expression of c-KIT protein was not detected in normal lung tissues. Since A549 cell is a human lung adenocarcinoma epithelial cell line, in the current study, we compared the expression levels of c-KIT in ADC with SCC, LCC, and SCLC.

The expression of c-KIT was elevated in 78 % (29/37) ADC and 71 % (36/51) SCC, whereas only 37 % (3/8) LCC showed increased expression of c-KIT (Fig. 6). A significant correlation was evident between the level of c-KIT expression and tumor type ($P = 0.046$), indicating that NSCLC tumor samples expressed higher levels of c-KIT compared to SCLC samples. In addition, Mann-Whitney *U* test analysis revealed that ADC tumor samples expressed higher levels of c-KIT compared to LCC ($P = 0.02$) and SCLC ($P = 0.02$) samples.

Discussion

Cancer stem cell theory implies that a distinct subset of cells with stem cell properties including self-renewal capacity, high resistance to chemotherapy, and radiation and metastasis potential are the main culprit in initiation and propagation of neoplasia, including lung cancer [2, 3, 35]. Although surface marker-based approach is the most widely used method for identification of CSCs, currently there is no universal consensus concerning the best CSC marker(s) for lung cancer [3, 8, 36]. In addition, the specificity and reliability of these markers for isolation of CSCs is not well established [8, 36]. Accordingly, sphere assays have been used for enrichment of CSCs in many tumor types [21, 36]. Thus, we enriched cancer stem-like cells in A549 cell line under non-adherent and SFM conditions, as described in our previous report [23]. Then the spheroid cells were characterized using colony-

Table 5 Important signaling pathways which are turned-on in the spheroid cells

Signaling pathways specific for embryonic stem cells		
Pathway	Gene name	Fold change (spheroid cells/ parental cells)
PI3K/AKT	CDK2	4.43
	IGF1R	3.15
	LPAR2	3.07
	PDPK1	2.85
	c-KIT	2.74
	PDGFRA	2.59
	BAD	2.28
	PRLR	2.27
	IKBKG	−2.02
	BCL2L1	−3.1
MAPK/ERK	RELB	4.06
	CDC25B	3.84
	MAP2K3	3.51
	DUSP3	2.68
	PDGFRA	2.59
	IKBKG	−2.02
JAK/STAT	TPO	3.18
	PRLR	2.27
	IL11	2.19
	SOCS2	2.15
	BCL2L1	−3.1
NF-kB	CXCL12	12.39
	RELB	4.06
	IKBKG	−2.02
	BCL2L1	−3.1
Hedgehog	SMO	2.46
Notch	PSEN	2.18
Signaling pathways related to epithelial-mesenchymal transition (EMT)		
Pathway	Gene name	Fold change
Ras	IGF1R	3.15
	c-KIT	2.74
	PDGFRA	2.59
	BAD	2.28
	IKBKG	−2.02
	RAB5C	−2.23
	BCL2L1	−3.1
Rap1	MAP2K3	3.51
	IGF1R	3.15
	LPAR2	3.07
	c-KIT	2.74
	CTNND1	2.72
	PDGFRA	2.59
AMPK	IGF1R	3.15
	PDPK1	2.85
	RAB10	2.05
	SIRT1	−2.07
TNF	MAP2K3	3.51
	RIPK3	2.58
	MMP14	2.16
	IKBKG	−2.02
Signaling pathways related to DNA repair		
Pathway	Gene name	Fold change
P53	CDK2	4.43
	DDB2	3.42
	PMAIP1	−2.22

forming assay and analysis of stemness markers at the gene and protein levels. Colony-formation assay of these cells revealed higher clonogenic capacity, larger size of colonies, and higher holoclone-forming ability, all considered to be cancer stem cell-like features [19, 37, 38]. Over-expression of Sox2 was also found in the spheroid cells compared to the parental cells, which is strongly related to the maintenance of stem cell properties and tumorigenesis potential of lung CSCs, as well as the enhancement of cellular invasion and anchorage-independent growth of these cells [39–42]. Notably, flow cytometric analysis of the spheroid cells indicated loss of CD44 expression and gain of CD24 expression ($CD44^{-}/CD24^{+}$) in spheroid cells which is in parallel with our previous report showing that $CD44^{+}/CD24^{+}$ and $CD44^{+}/CD24^{-/low}$ subpopulations do not represent CSC subpopulation of A549 cells [23]. The CD44/CD24 phenotype has not been previously investigated in lung cancer clinical samples, but a report by Jaggupilli et al. indicated no expression of both potential markers CD44 and CD24 in NSCLC cell line COR L23 [43]. Evaluation of CD44/CD24 phenotype in other cancer types has suggested a subpopulation of $CD44^{+}/CD24^{-/low}$ cells as breast CSCs population, and $CD44^{+}/CD24^{+}$ phenotype as potential CSC marker in ovarian, pancreatic, and colorectal cancer [44–47]. Therefore, expression of CD44 and CD24 is highly variable in various cancer cell lines and tissues, including lung cancer. The $CD44^{+}/CD24^{-/low}$ correlates with better survival and $CD44^{-}/CD24^{+}$ and $CD44^{-}/CD24^{-/low}$ phenotypes correlate with poor prognosis and shorter survival in breast cancer patients [48–50]. Collectively, these data demonstrated that the spheroid cells derived from A549 cells can be considered as a cancer stem-like cell population [35, 37, 38, 51].

Monitoring of gene expression profiling demonstrated that 160 genes were differentially expressed between the spheroid cells as cancer stem-like cells and parental cells as low tumorigenic cells. The list of DEGs was categorized into three main groups; the first group contains genes involved in PI3K/AKT, MAPK/ERK, JAK/STAT, NF-κB, Wnt, TGF-β, Hedgehog, and Notch signaling pathways. All of these networks have been previously identified as embryonic stem cell (ESC)-associated signaling pathways [52, 53], which implies that CSCs

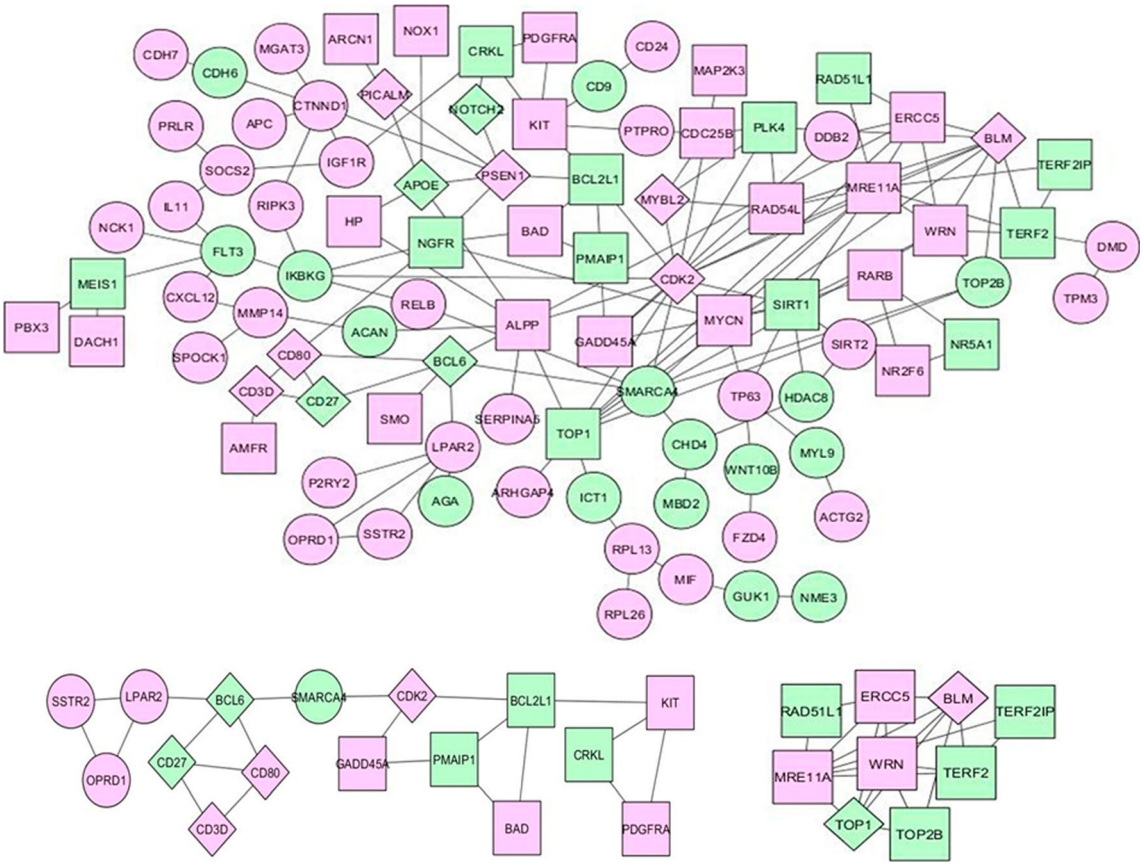

Fig. 4 Protein-protein interactions (PPI) network and the important sub-networks of differentially expressed genes (DEGs) in the spheroid cells reconstructed using STRING database. PPI networks are presented in an undirected graph format, with nodes (red nodes = up-regulated genes and green nodes = down-regulated genes) corresponding to proteins; and edges corresponding to physical protein-protein interactions

can originate from ESCs. Although some observations support the notion that the accumulation of DNA damage hits and later genetic reprogramming may convert normal stem cells to CSCs, currently there is no consensus regarding the origin of CSCs [54–58].

Our findings demonstrated that PI3K/AKT is the most important signaling pathway in the spheroid cells as cancer stem-like cells and its effects are mediated through the activation of NF-κB pathways (Fig. 3), which is consistent with previous reports in acute malignant leukemia and breast and prostate

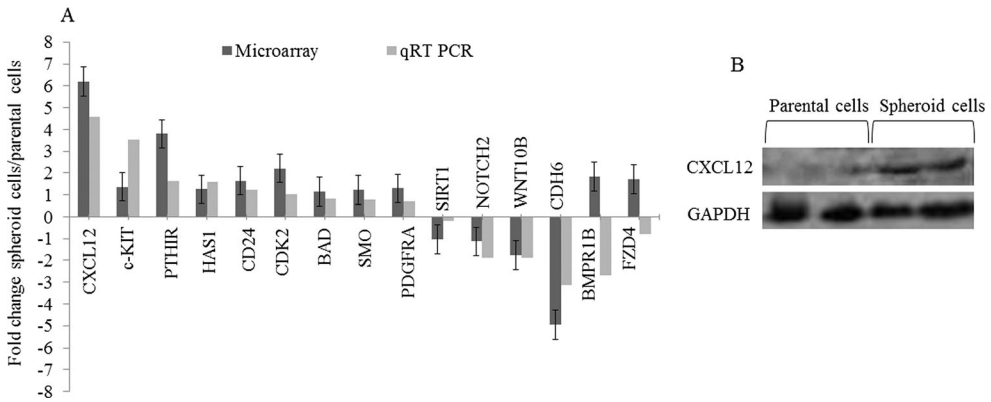

Fig. 5 Validation of microarray data using **a** qRT-PCR analysis: validation of average gene expression changes in the spheroid cells as compared to the parental cells when detected by microarray technique (*black bar*) and qRT-PCR analysis (*gray bar*). **b** Western blots analysis of CXCL12 protein expression. Equal amounts of protein from total cell lysates of parental cells and the spheroid cells were loaded and analyzed using antibodies against CXCL12. GAPDH was used as an internal control

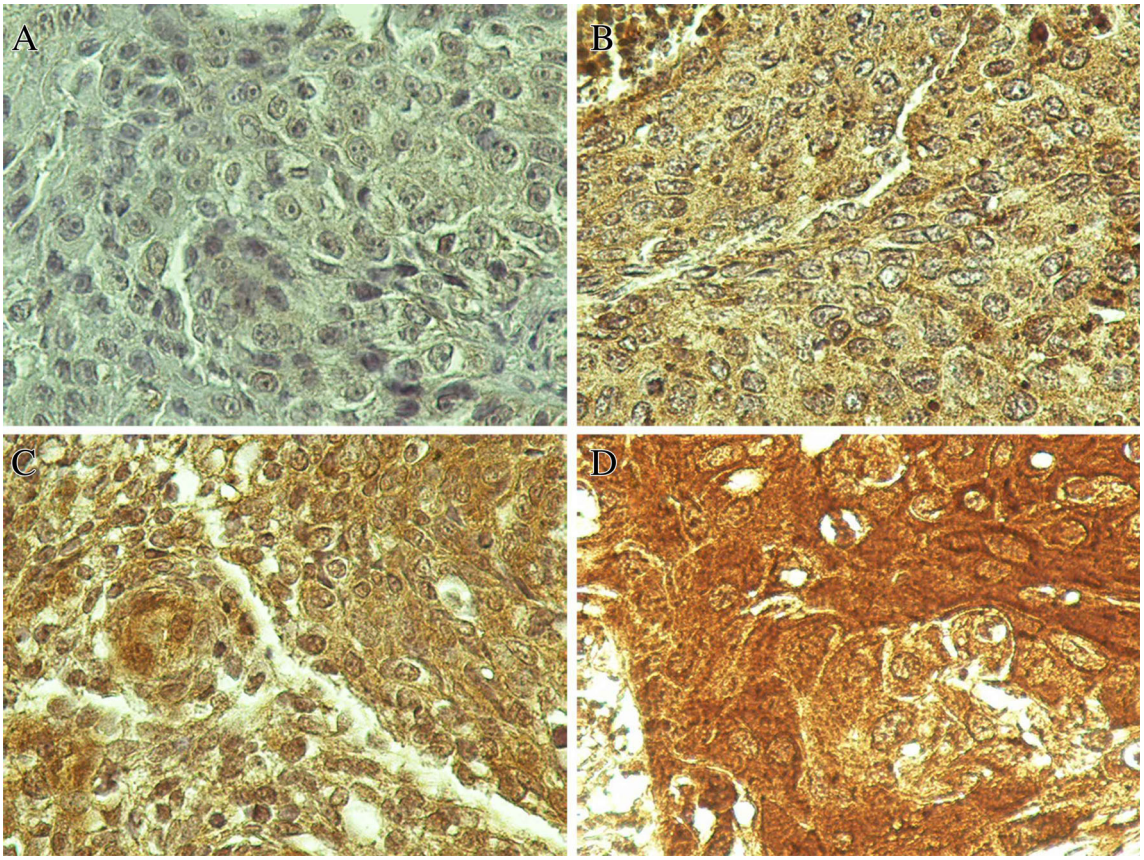

Fig. 6 Representative photographs of the immunohistochemical staining of c-KIT from lung cancer patients. **a** 0 = no staining. **b** +1 = weak. **c** +2 = moderate. **d** +3 = strong intensity of staining (×200 magnification)

CSCs [59–61]. Subsequently, we showed that activation of the NF-κB pathway causes over-expression of CXCL12 which was the most highly up-regulated gene in the spheroid cells in our current study (12.3-fold) (Fig. 3). CXCL12 binds to CXC receptor 4 (CXCR4) and leads to activation of the PI3K/AKT-NF-κB axis and thus facilitates angiogenesis, tumor progression and metastasis [34].

Prior research implies that expression of CXCR4 regulates CXCL12 expression which in turn enhances aggressive tumor behavior and metastasis in NSCLC, and knockdown of this axis can be considered as a potential therapeutic target [62, 63]. Additionally, activation of PI3K/AKT pathway in our spheroid cells was parallel with increased expression of CDK2 and BAD molecules and decreased expression of Bcl-xL (Fig. 3) which leads to apoptosis [64]. Similar to studies in breast and ovarian CSCs [65–67], activation of MAPK/ERK and JAK/STAT pathways was detected in our spheroid cells (Fig. 3) which supports the notion that these pathways promote cancer stem-like cell properties. Up-regulation of PI3K/AKT, MAPK/ERK, and NF-κB pathways are responsible for ESCs' pluripotency [68].

In the second gene group, we found DEGs which are part of Ras, Rap1, AMPK, and TNF pathways and EMT process which are implicated in cancer migration, invasion, and metastasis [69–75]. In this group, Ras pathway is the most important cellular pathway, which promotes cytoskeletal remodeling through RAB5C (Fig. 3). Activation of both the RAS and PI3K/AKT pathways was found in our spheroid cells which are reported to accelerate tumor progression and metastasis in prostate CSCs [71]. Activation of Rap1 pathway in spheroid cells was observed which lead to increased expression of CTNND1 and MAP2K3 (Fig. 3). Activation of Rap1 pathway and over-expression of CXCL12 in our study is similar to previous reports implying that activation of Rap1 pathway promotes cell proliferation and metastatic progression in several tumor types including melanoma, pancreas, and prostate cancer, which in turn lead to the over-expression of CXCL12 [69, 73–75]. We also found the over-expression of MMP14 in the context of TNF pathway (Fig. 3), a pattern that has been shown to lead to the disruption of the extracellular matrix and provide a unique environment for cell migration and metastasis [72]. Furthermore, we found the over-expression of several DEGs with key roles in the EMT process, including c-KIT (threefold), IGF1R (threefold), PDGFRA (2.6-fold), Annexin 2 (2.5-fold), MMP14 (two-fold), and low expression of CDH6 (tenfold). EMT is controlled by a complex network of events during tumorigenesis that orchestrate cells for migration to distant sites, thus

forming metastatic foci [76, 77]. Our findings demonstrated increased activity of PI3/AKT, MAPK/AEK, Hedgehog, Notch, Ras, and NF-κB signaling pathways in spheroid cells that confirm previous studies suggesting these pathways may contribute to the EMT process [78–80]. In addition, a noticeable decrease in CDH6 expression, a membrane-bound glycoprotein involved in the adherence of adjacent cells, was detected in spheroid cells in our study; which is known to be a critical step in promoting EMT [81, 82]. Also, it is shown that the loss of E-cadherins, including CDH6 in primary tumors is related to tumor metastasis and poor prognosis in lung cancer patients [83, 84].

RAB GTPases family facilitates exosome formation and mediates intercellular communications [85, 86]. Of note, high expression of several elements of RAB GTPases family including RAB27a (3.5-fold), RAB36 (2.4-fold), and RAB10 (twofold) was seen in spheroid cells. Some previous studies have shown that exosomes-derived CSCs could be involved in angiogenesis, pre-metastatic niche formation, tumor progression, and metastasis [85, 86].

Additionally, our study showed the elevated expression of carcinoembryonic antigen-related cell adhesion molecule 1 (CEACAM1) (3.86-fold) in the spheroid cells; overexpression of CEACAM1 in breast CSCs correlate with angiogenesis and metastasis potential, as well as promotion of invasion and recurrence of colon cancer and hepatocellular carcinoma [87–89]. Expression of CD24, associated with tumor progression and metastasis [43, 90], was also upregulated (3.2-fold) in spheroid cells. In addition to the diagnostic and prognostic values, CD24 when co-expressed along with other putative markers such as CD44 and CD29 has been used for isolating CSCs from various tumors [54, 91, 92].

We also explored the probable interactions among DEGs with reconstructing the PPI network for the studied genes, considering that finding reliable sub-network markers can help in assessing the tumorigenecity, biomarker discovery, and also more accurate classification of cancer [93, 94]. CDK2, as a stopping point for G1/S phase transition, was located at the core of the network; over-expression of CDK2 is shown to be involved in the maintenance of pluripotency of stem cells [95]. MRE11A, a component of MRN complex as major sensor of DNA double-strand breaks, was the second most important molecule in the spheroid cells' PPI network [96]. MRN complex is related to carcinogenesis, aggressive tumor behavior, induction of EMT, and poor prognosis [97–101]. Additionally, we found simultaneous overexpression of MRE11A and activation of PI3/AKT pathway in the spheroid cells; this pattern is previously reported to correlate with higher content of CSCs in various tumors [96].

The well-known characteristics of CSCs are long-term self-renewal capacity, multilineage differentiation, resistance to apoptosis, and drug resistance. This phenotype is tightly orchestrated by multiple regulatory networks and mediated by interaction or crosstalk between them, as well as the cancer cell microenvironment [102, 103]. Our results are highly suggestive of crosstalk between the dedifferentiation pathways which confer maintenance of self-renewal and pluripotency features to tumors, including the CSC subpopulation of tumors and that of the pathways associated with tumor aggressiveness, distant metastatic seeding, and EMT which are features commonly attributed to the CSC subpopulation of tumors.

Our gene expression data was validated at the gene level using qRT-PCR analysis which showed a robust correlation with cDNA microarray data. The expression levels of BMPR1B and FZD4 in cDNA microarray analysis were changing in opposite directions as compared to the results of qRT-PCR analysis; however, this discrepancy was not statistically significant.

Our immunohistochemical analysis showed no expression of c-KIT in lung tissues and highest expression of c-KIT was found in ADC of lung compared with other subtypes of lung tumors. These data implies that c-KIT may be considered as potential molecule for targeted therapy in lung cancer, especially for ADC. There is no consensus among the previously published reports concerning the c-KIT expression in lung cancer [104–107]. Levina et al. showed the significant role of c-Kit in self-renewal of lung CSCs and its potential role in targeted therapy [104]. Moreover, some studies have shown that c-KIT can be a negative prognostic factor in NSCLC; other studies demonstrated that there is no association between c-KIT and SCLC tumor progression [105–107].

Conclusions

Embryonic stem cell-like gene expression signature of the spheroid cells strongly support the notion that maintenance of CSCs phenotype is achieved by dedifferentiating mechanisms activated through tumor-specific signaling pathways, and also support the hypothesis that CSCs are originated from ESCs. Additionally, increased activity of PI3/AKT, as the most prominently up-regulated pathway, and other pathways related to tumor progression, aggressiveness, and EMT in the spheroid cells imply that CSCs are indeed involved in tumor metastasis and seeding to distant organs. Of note, PPI network analysis revealed robust activation of some key proteins related to DNA damage repair in the spheroid cells, including MRE11A. The above-mentioned findings can pave the way for drug discovery and targeted therapy of lung cancer by identifying the specific molecular pathways in CSCs, inactivation of which can lead to the highest degree of tumor regression and therapeutic gain.

Acknowledgments This study was performed for the fulfillment of Ph.D dissertation requirements (R.R.) and was supported by Iran University of Medical Sciences (Grant no #1030) and Royan Institute for Stem Cell Biology and Technology (Grant no # p-90-153).

Compliance with ethical standards

Conflicts of interest None

References

1. Jemal A, Bray F, Center MM, Ferlay J, Ward E, Forman D. Global cancer statistics. CA Cancer J Clin. 2011;61(2):69–90. doi:10.3322/caac.20107.
2. Wang J, Li Z-H, White J, Zhang L-B. Lung cancer stem cells and implications for future therapeutics. Cell Biochem Biophys. 2014;69(3):389–98. doi:10.1007/s12013-014-9844-4.
3. Alamgeer M, Peacock CD, Matsui W, Ganju V, Watkins DN. Cancer stem cells in lung cancer: evidence and controversies. Respirology. 2013;18(5):757–64. doi:10.1111/resp.12094.
4. Azizi E, Wicha MS. Point: cancer stem cells—the evidence accumulates. Clin Chem. 2013;59(1):205–7. doi:10.1373/clinchem.2012.195990.
5. Shukla S, Meeran SM. Epigenetics of cancer stem cells: pathways and therapeutics. Biochim Biophys Acta. 2014;1840(12):3494–502. doi:10.1016/j.bbagen.2014.09.017.
6. Perumal D, Singh S, Yoder SJ, Bloom GC, Chellappan SP. A novel five gene signature derived from stem-like side population cells predicts overall and recurrence-free survival in NSCLC. PLoS One. 2012;7(8), e43589. doi:10.1371/journal.pone.0043589.
7. Seo D-C, Sung J-M, Cho H-J, Yi H, Seo K-H, Choi I-S, et al. Gene expression profiling of cancer stem cell in human lung adenocarcinoma A549 cells. Mol Cancer. 2007;6(1):75.
8. Dou J, Gu N. Emerging strategies for the identification and targeting of cancer stem cells. Tumor Biol. 2010;31(4):243–53. doi:10.1007/s13277-010-0023-y.
9. Bertolini G, Roz L, Perego P, Tortoreto M, Fontanella E, Gatti L, et al. Highly tumorigenic lung cancer CD133+ cells display stem-like features and are spared by cisplatin treatment. Proc Natl Acad Sci U S A. 2009;106(38):16281–6. doi:10.1073/pnas.0905653106.
10. Chen Y-C, Hsu H-S, Chen Y-W, Tsai T-H, How C-K, Wang C-Y, et al. Oct-4 expression maintained cancer stem-like properties in lung cancer-derived CD133-positive cells. PLoS One. 2008;3(7), e2637. doi:10.1371/journal.pone.0002637.
11. Eramo A, Lotti F, Sette G, Pilozzi E, Biffoni M, Di Virgilio A, et al. Identification and expansion of the tumorigenic lung cancer stem cell population. Cell Death Differ. 2007;15(3):504–14.
12. Ho MM, Ng AV, Lam S, Hung JY. Side population in human lung cancer cell lines and tumors is enriched with stem-like cancer cells. Cancer Res. 2007;67(10):4827–33.
13. Jiang F, Qiu Q, Khanna A, Todd NW, Deepak J, Xing L, et al. Aldehyde dehydrogenase 1 is a tumor stem cell-associated marker in lung cancer. Mol Cancer Res. 2009;7(3):330–8. doi:10.1158/1541-7786.MCR-08-0393.
14. Leung EL-H, Fiscus RR, Tung JW, Tin VP-C, Cheng LC, Sihoe AD-L, et al. Non-small cell lung cancer cells expressing CD44 are enriched for stem cell-like properties. PLoS One. 2010;5(11), e14062. doi:10.1371/journal.pone.0014062.
15. Meng X, Li M, Wang X, Wang Y, Ma D. Both CD133+ and CD133- subpopulations of A549 and H446 cells contain cancer-initiating cells. Cancer Sci. 2009;100(6):1040–6. doi:10.1111/j.1349-7006.2009.01144.x.
16. Shi Y, Fu X, Hua Y, Han Y, Lu Y, Wang J. The side population in human lung cancer cell line NCI-H460 is enriched in stem-like cancer cells. PLoS One. 2012;7(3), e33358. doi:10.1371/journal.pone.0033358.
17. Wang P, Gao Q, Suo Z, Munthe E, Solberg S, Ma L, et al. Identification and characterization of cells with cancer stem cell properties in human primary lung cancer cell lines. PLoS One. 2013;8(3), e57020. doi:10.1371/journal.pone.0057020.
18. Liu J, Xiao Z, Wong SK-M, Tin VP-C, Ho K-Y, Wang J, et al. Lung cancer tumorigenicity and drug resistance are enhanced through ALDH (hi) CD44 (hi) tumor initiating cells. Oncotarget. 2013;4(10):1698–711.
19. Cao L, Zhou Y, Zhai B, Liao J, Xu W, Zhang R, et al. Sphere-forming cell subpopulations with cancer stem cell properties in human hepatoma cell lines. BMC Gastroenterol. 2011;11(1):71. doi:10.1186/1471-230X-11-71.
20. Liu J, Ma L, Wang Z, Wang L, Liu C, Chen R, et al. MicroRNA expression profile of gastric cancer stem cells in the MKN-45 cancer cell line. Acta Biochim Biophys Sin Shanghai. 2014;46(2):92–9. doi:10.1093/abbs/gmt135.
21. Pastrana E, Silva-Vargas V, Doetsch F. Eyes wide open: a critical review of sphere-formation as an assay for stem cells. Cell Stem Cell. 2011;8(5):486–98. doi:10.1016/j.stem.2011.04.007.
22. Singh SK, Clarke ID, Terasaki M, Bonn VE, Hawkins C, Squire J, et al. Identification of a cancer stem cell in human brain tumors. Cancer Res. 2003;63(18):5821–8.
23. Roudi R, Madjd Z, Ebrahimi M, Samani FS, Samadikuchaksaraei A. CD44 and CD24 cannot act as cancer stem cell markers in human lung adenocarcinoma cell line A549. Cell Mol Biol Lett. 2014;19(1):23–36. doi:10.2478/s11658-013-0112-1.
24. Yang YH, Dudoit S, Luu P, Lin DM, Peng V, Ngai J, et al. Normalization for cDNA microarray data: a robust composite method addressing single and multiple slide systematic variation. Nucleic Acids Res. 2002;30(4), e15-e.
25. Jensen LJ, Kuhn M, Stark M, Chaffron S, Creevey C, Muller J, et al. STRING 8—a global view on proteins and their functional interactions in 630 organisms. Nucleic Acids Res. 2009;37 suppl 1:D412–6. doi:10.1093/nar/gkn760.
26. Kanehisa M, Goto S. KEGG: Kyoto encyclopedia of genes and genomes. Nucleic Acids Res. 2000;28(1):27–30.
27. Joshi-Tope G, Gillespie M, Vastrik I, D'Eustachio P, Schmidt E, de Bono B, et al. Reactome: a knowledgebase of biological pathways. Nucleic Acids Res. 2005;33 suppl 1:D428–32.
28. Nishimura D. BioCarta. Biotech Software & Internet Report: The Computer Software Journal for Scient. 2001;2(3):117–20.
29. Roudi R, Madjd Z, Korourian A, Mehrazma M, Molanae S, Sabet MN, et al. Clinical significance of putative cancer stem cell marker CD44 in different histological subtypes of lung cancer. Cancer Biomark. 2014;14(6):457–67. doi:10.3233/CBM-140424.
30. Roudi R, Korourian A, Shariftabrizi A, Madjd Z. Differential expression of cancer stem cell markers ALDH1 and CD133 in various lung cancer subtypes. Cancer Investig. 2015;33(7):294–302. doi:10.3109/07357907.2015.1034869.
31. McCarty Jr K, Miller L, Cox E, Konrath J, McCarty Sr K. Estrogen receptor analyses. Correlation of biochemical and immunohistochemical methods using monoclonal antireceptor antibodies. Arch Pathol Lab Med. 1985;109(8):716–21.
32. Povey S, Lovering R, Bruford E, Wright M, Lush M, Wain H. The HUGO gene nomenclature committee (HGNC). Hum Genet. 2001;109(6):678–80.
33. Dennis Jr G, Sherman BT, Hosack DA, Yang J, Gao W, Lane HC, et al. DAVID: database for annotation, visualization, and integrated discovery. Genome Biol. 2003;4(5):3.

34. Teicher BA, Fricker SP. CXCL12 (SDF-1)/CXCR4 pathway in cancer. Clin Cancer Res. 2010;16(11):2927–31. doi:10.1158/1078-0432.CCR-09-2329.
35. Clevers H. The cancer stem cell: premises, promises and challenges. Nat Med. 2011;17(3):313–9. doi:10.1038/nm.2304.
36. J-j D, Qiu W, Xu S-l, Wang B, X-z Y, Y-f P, et al. Strategies for isolating and enriching cancer stem cells: well begun is half done. Stem Cells Dev. 2013;22(16):2221–39. doi:10.1089/scd.2012.0613.
37. Castillo V, Valenzuela R, Huidobro C, Contreras HR, Castellon EA. Functional characteristics of cancer stem cells and their role in drug resistance of prostate cancer. Int J Oncol. 2014;45(3):985–94. doi:10.3892/ijo.2014.2529.
38. Ciliberto G. Mammosphere-forming cells from breast cancer cell lines as a tool for the identification of CSC-like and early progenitor-targeting drugs. Cell Cycle. 2010;9(14):2878–87.
39. Xiang R, Liao D, Cheng T, Zhou H, Shi Q, Chuang T, et al. Downregulation of transcription factor SOX2 in cancer stem cells suppresses growth and metastasis of lung cancer. Br J Cancer. 2011;104(9):1410–7. doi:10.1038/bjc.2011.94.
40. Chen S, Xu Y, Chen Y, Li X, Mou W, Wang L, et al. SOX2 gene regulates the transcriptional network of oncogenes and affects tumorigenesis of human lung cancer cells. PLoS One. 2012;7(5), e36326. doi:10.1371/journal.pone.0036326.
41. Singh S, Trevino J, Bora-Singhal N, Coppola D, Haura E, Altiok S, et al. EGFR/Src/Akt signaling modulates Sox2 expression and self-renewal of stem-like side-population cells in non-small cell lung cancer. Mol Cancer. 2012;11(1):73. doi:10.1186/1476-4598-11-73.
42. Hussenet T, Dali S, Exinger J, Monga B, Jost B, Dembelé D, et al. SOX2 is an oncogene activated by recurrent 3q26. 3 amplifications in human lung squamous cell carcinomas. PLoS One. 2010;5(1), e8960. doi:10.1371/journal.pone.0008960.
43. Jaggupilli A, Elkord E. Significance of CD44 and CD24 as cancer stem cell markers: an enduring ambiguity. J Immunol Res/Clin Dev Immunol. 2012;2012:708036. doi:10.1155/2012/708036.
44. Al-Hajj M, Wicha MS, Benito-Hernandez A, Morrison SJ, Clarke MF. Prospective identification of tumorigenic breast cancer cells. Proc Natl Acad Sci U S A. 2003;100(7):3983–8.
45. Wei X, Dombkowski D, Meirelles K, Pieretti-Vanmarcke R, Szotek PP, Chang HL, et al. Müllerian inhibiting substance preferentially inhibits stem/progenitors in human ovarian cancer cell lines compared with chemotherapeutics. Proc Natl Acad Sci U S A. 2010;107(44):18874–9. doi:10.1073/pnas.1012667107.
46. Li C, Heidt DG, Dalerba P, Burant CF, Zhang L, Adsay V, et al. Identification of pancreatic cancer stem cells. Cancer Res. 2007;67(3):1030–7.
47. Collins AT, Berry PA, Hyde C, Stower MJ, Maitland NJ. Prospective identification of tumorigenic prostate cancer stem cells. Cancer Res. 2005;65(23):10946–51.
48. Adamczyk A, Niemiec JA, Ambicka A, Mucha-Małecka A, Mituś J, Ryś J. CD44/CD24 as potential prognostic markers in node-positive invasive ductal breast cancer patients treated with adjuvant chemotherapy. J Mol Histol. 2014;45(1):35–45. doi:10.1007/s10735-013-9523-6.
49. Ahmed MA, Aleskandarany MA, Rakha EA, Moustafa RZ, Benhasouna A, Nolan C, et al. A CD44−/CD24+ phenotype is a poor prognostic marker in early invasive breast cancer. Breast Cancer Res Treat. 2012;133(3):979–95. doi:10.1007/s10549-011-1865-8.
50. Mylona E, Giannopoulou I, Fasomytakis E, Nomikos A, Magkou C, Bakarakos P, et al. The clinicopathologic and prognostic significance of CD44+/CD24−/low and CD44−/CD24+ tumor cells in invasive breast carcinomas. Hum Pathol. 2008;39(7):1096–102. doi:10.1016/j.humpath.2007.12.003.
51. Singh SK, Hawkins C, Clarke ID, Squire JA, Bayani J, Hide T, et al. Identification of human brain tumour initiating cells. Nature. 2004;432(7015):396–401.
52. Dreesen O, Brivanlou AH. Signaling pathways in cancer and embryonic stem cells. Stem Cell Rev. 2007;3(1):7–17.
53. Han L, Shi S, Gong T, Zhang Z, Sun X. Cancer stem cells: therapeutic implications and perspectives in cancer therapy. Acta Pharm Sin B. 2013;3(2):65–75.
54. Al-Hajj M, Becker MW, Wicha M, Weissman I, Clarke MF. Therapeutic implications of cancer stem cells. Curr Opin Genet Dev. 2004;14(1):43–7.
55. Ratajczak MZ. Cancer stem cells-normal stem cells "Jedi" that went over to the "dark side". Folia Histochem Cytobiol. 2005;43(4):175–81.
56. Reya T, Duncan AW, Ailles L, Domen J, Scherer DC, Willert K, et al. A role for Wnt signalling in self-renewal of haematopoietic stem cells. Nature. 2003;423(6938):409–14.
57. Soltanian S, Matin MM. Cancer stem cells and cancer therapy. Tumour Biol. 2011;32(3):425–40. doi:10.1007/s13277-011-0155-8.
58. Bjerkvig R, Tysnes BB, Aboody KS, Najbauer J, Terzis AJA. The origin of the cancer stem cell: current controversies and new insights. Nat Rev Cancer. 2005;5(11):899–904.
59. Martelli AM, Nyåkern M, Tabellini G, Bortul R, Tazzari PL, Evangelisti C, et al. Phosphoinositide 3-kinase/Akt signaling pathway and its therapeutical implications for human acute myeloid leukemia. Leukemia. 2006;20(6):911–28.
60. Dillon RL, White DE, Muller WJ. The phosphatidyl inositol 3-kinase signaling network: implications for human breast cancer. Oncogene. 2007;26(9):1338–45.
61. Dubrovska A, Kim S, Salamone RJ, Walker JR, Maira S-M, García-Echeverría C, et al. The role of PTEN/Akt/PI3K signaling in the maintenance and viability of prostate cancer stem-like cell populations. Proc Natl Acad Sci U S A. 2009;106(1):268–73. doi:10.1073/pnas.0810956106.
62. Choi YH, Burdick MD, Strieter BA, Mehrad B, Strieter RM. CXCR4, but not CXCR7, discriminates metastatic behavior in non–small cell lung cancer cells. Mol Cancer Res. 2014;12(1):38–47. doi:10.1158/1541-7786.MCR-12-0334.
63. Liu Y, Wu BQ, Geng H, Xu ML, Zhong HH. Association of chemokine and chemokine receptor expression with the invasion and metastasis of lung carcinoma. Oncol Lett. 2015;10(3):1315–22.
64. Wafa K. The role of a Cyclin D2 splice variant in the regulation of the cell cycle: connecting cell cycle to cancer biology. 2014.
65. Abubaker K, Luwor RB, Escalona R, McNally O, Quinn MA, Thompson EW, et al. Targeted disruption of the JAK2/STAT3 pathway in combination with systemic administration of paclitaxel inhibits the priming of ovarian cancer stem cells leading to a reduced tumor burden. Front Oncol. 2014;4:75. doi:10.3389/fonc.2014.00075.
66. Abubaker K, Luwor RB, Zhu H, McNally O, Quinn MA, Burns CJ, et al. Inhibition of the JAK2/STAT3 pathway in ovarian cancer results in the loss of cancer stem cell-like characteristics and a reduced tumor burden. BMC Cancer. 2014;14:317. doi:10.1186/1471-2407-14-317.
67. Balko JM, Schwarz LJ, Bhola NE, Kurupi R, Owens P, Miller TW, et al. Activation of MAPK pathways due to DUSP4 loss promotes cancer stem cell-like phenotypes in basal-like breast cancer. Cancer Res. 2013;73(20):6346–58. doi:10.1158/0008-5472.CAN-13-1385.
68. Armstrong L, Hughes O, Yung S, Hyslop L, Stewart R, Wappler I, et al. The role of PI3K/AKT, MAPK/ERK and NFκβ signalling in the maintenance of human embryonic stem cell pluripotency and viability highlighted by transcriptional profiling and functional analysis. Hum Mol Genet. 2006;15(11):1894–913.

69. Hattori M, Minato N. Rap1 GTPase: functions, regulation, and malignancy. J Biochem. 2003;134(4):479–84.
70. Morel A-P, Lièvre M, Thomas C, Hinkal G, Ansieau S, Puisieux A. Generation of breast cancer stem cells through epithelial-mesenchymal transition. PLoS One. 2008;3(8), e2888. doi:10.1371/journal.pone.0002888.
71. Mulholland DJ, Kobayashi N, Ruscetti M, Zhi A, Tran LM, Huang J, et al. Pten loss and RAS/MAPK activation cooperate to promote EMT and metastasis initiated from prostate cancer stem/progenitor cells. Cancer Res. 2012;72(7):1878–89. doi:10.1158/0008-5472.CAN-11-3132.
72. Singh A, Settleman J. EMT, cancer stem cells and drug resistance: an emerging axis of evil in the war on cancer. Oncogene. 2010;29(34):4741–51. doi:10.1038/onc.2010.215.
73. Bailey CL, Kelly P, Casey PJ. Activation of Rap1 promotes prostate cancer metastasis. Cancer Res. 2009;69(12):4962–8. doi:10.1158/0008-5472.CAN-08-4269.
74. Gao L, Feng Y, Bowers R, Becker-Hapak M, Gardner J, Council L, et al. Ras-associated protein-1 regulates extracellular signal-regulated kinase activation and migration in melanoma cells: two processes important to melanoma tumorigenesis and metastasis. Cancer Res. 2006;66(16):7880–8.
75. Zhang L, Chenwei L, Mahmood R, van Golen K, Greenson J, Li G, et al. Identification of a putative tumor suppressor gene Rap1GAP in pancreatic cancer. Cancer Res. 2006;66(2):898–906.
76. Hollier BG, Evans K, Mani SA. The epithelial-to-mesenchymal transition and cancer stem cells: a coalition against cancer therapies. J Mammary Gland Biol Neoplasia. 2009;14(1):29–43. doi:10.1007/s10911-009-9110-3.
77. Scheel C, Weinberg RA. Cancer stem cells and epithelial–mesenchymal transition: concepts and molecular links. Semin Cancer Biol. 2012;22(5–6):396–403. doi:10.1016/j.semcancer.2012.04.001.
78. Kalluri R, Weinberg RA. The basics of epithelial-mesenchymal transition. J Clin Invest. 2009;119(6):1420–8. doi:10.1172/JCI39104.
79. Zavadil J, Haley J, Kalluri R, Muthuswamy SK, Thompson E. Epithelial-mesenchymal transition. Cancer Res. 2008;68(23):9574–7. doi:10.1158/0008-5472.CAN-08-2316.
80. Huber MA, Kraut N, Beug H. Molecular requirements for epithelial–mesenchymal transition during tumor progression. Curr Opin Cell Biol. 2005;17(5):548–58.
81. Onder TT, Gupta PB, Mani SA, Yang J, Lander ES, Weinberg RA. Loss of E-cadherin promotes metastasis via multiple downstream transcriptional pathways. Cancer Res. 2008;68(10):3645–54. doi:10.1158/0008-5472.CAN-07-2938.
82. Ye Y, Xiao Y, Wang W, Yearsley K, Gao J, Shetuni B, et al. ERα signaling through slug regulates E-cadherin and EMT. Oncogene. 2010;29(10):1451–62. doi:10.1038/onc.2009.433.
83. Deeb G, Wang J, Ramnath N, Slocum HK, Wiseman S, Beck A, et al. Altered E-cadherin and epidermal growth factor receptor expressions are associated with patient survival in lung cancer: a study utilizing high-density tissue microarray and immunohistochemistry. Mod Pathol. 2004;17(4):430–9.
84. Bremnes R, Veve R, Gabrielson E, Hirsch F, Baron A, Bemis L, et al. High-throughput tissue microarray analysis used to evaluate biology and prognostic significance of the E-cadherin pathway in non–small-cell lung cancer. J Clin Oncol. 2002;20(10):2417–28.
85. Kahlert C, Kalluri R. Exosomes in tumor microenvironment influence cancer progression and metastasis. J Mol Med (Berl). 2013;91(4):431–7. doi:10.1007/s00109-013-1020-6.
86. Grange C, Tapparo M, Collino F, Vitillo L, Damasco C, Deregibus MC, et al. Microvesicles released from human renal cancer stem cells stimulate angiogenesis and formation of lung premetastatic niche. Cancer Res. 2011;71(15):5346–56. doi:10.1158/0008-5472.CAN-11-0241.
87. Kiriyama S, Yokoyama S, Ueno M, Hayami S, Ieda J, Yamamoto N, et al. CEACAM1 long cytoplasmic domain isoform is associated with invasion and recurrence of hepatocellular carcinoma. Ann Surg Oncol. 2014;21 Suppl 4:S505–14. doi:10.1245/s10434-013-3460-1.
88. Bajenova O, Chaika N, Tolkunova E, Davydov-Sinitsyn A, Gapon S, Thomas P, et al. Carcinoembryonic antigen promotes colorectal cancer progression by targeting adherens junction complexes. Exp Cell Res. 2014;324(2):115–23. doi:10.1016/j.yexcr.2014.04.007.
89. Wang K-H, Kao A-P, Chang C-C, Lee J-N, Hou M-F, Long C-Y, et al. Increasing CD44+/CD24-tumor stem cells, and upregulation of COX-2 and HDAC6, as major functions of HER2 in breast tumorigenesis. Mol Cancer. 2010;9:288. doi:10.1186/1476-4598-9-288.
90. Visvader JE, Lindeman GJ. Cancer stem cells in solid tumours: accumulating evidence and unresolved questions. Nat Rev Cancer. 2008;8(10):755–68. doi:10.1038/nrc2499.
91. Hurt EM, Kawasaki BT, Klarmann GJ, Thomas SB, Farrar WL. CD44+ CD24− prostate cells are early cancer progenitor/stem cells that provide a model for patients with poor prognosis. Br J Cancer. 2008;98(4):756–65. doi:10.1038/sj.bjc.6604242.
92. Yeung TM, Gandhi SC, Wilding JL, Muschel R, Bodmer WF. Cancer stem cells from colorectal cancer-derived cell lines. Proc Natl Acad Sci U S A. 2010;107(8):3722–7. doi:10.1073/pnas.0915135107.
93. Su J, Yoon B-J, Dougherty ER. Identification of diagnostic subnetwork markers for cancer in human protein-protein interaction network. BMC Bioinformatics. 2010;11 Suppl 6:S8–9. doi:10.1186/1471-2105-11-S6-S8.
94. Wu G, Feng X, Stein L. A human functional protein interaction network and its application to cancer data analysis. Genome Biol. 2010;11(5):R53. doi:10.1186/gb-2010-11-5-r53.
95. Lin S-L, Chang DC, Ying S-Y, Leu D, Wu DT. MicroRNA miR-302 inhibits the tumorigenecity of human pluripotent stem cells by coordinate suppression of the CDK2 and CDK4/6 cell cycle pathways. Cancer Res. 2010;70(22):9473–82. doi:10.1158/0008-5472.CAN-10-2746.
96. Skvortsov S, Debbage P, Lukas P, Skvortsova I. Crosstalk between DNA repair and cancer stem cell (CSC) associated intracellular pathways. Semin Cancer Biol. 2015;31:36–42. doi:10.1016/j.semcancer.2014.06.002.
97. Skvortsova I, Skvortsov S, Stasyk T, Raju U, Popper BA, Schiestl B, et al. Intracellular signaling pathways regulating radioresistance of human prostate carcinoma cells. Proteomics. 2008;8(21):4521–33. doi:10.1002/pmic.200800113.
98. Yang MH, Chang SY, Chiou SH, Liu CJ, Chi CW, Chen PM, et al. Overexpression of NBS1 induces epithelial–mesenchymal transition and co-expression of NBS1 and Snail predicts metastasis of head and neck cancer. Oncogene. 2007;26(10):1459–67.
99. Yang M-H, Chiang W-C, Chou T-Y, Chang S-Y, Chen P-M, Teng S-C, et al. Increased NBS1 expression is a marker of aggressive head and neck cancer and overexpression of NBS1 contributes to transformation. Clin Cancer Res. 2006;12(2):507–15.
100. Chen Y-C, Su Y-N, Chou P-C, Chiang W-C, Chang M-C, Wang L-S, et al. Overexpression of NBS1 contributes to transformation through the activation of phosphatidylinositol 3-kinase/Akt. J Biol Chem. 2005;280(37):32505–11.
101. Cheng L, Wu Q, Huang Z, Guryanova OA, Huang Q, Shou W, et al. L1CAM regulates DNA damage checkpoint response of glioblastoma stem cells through NBS1. EMBO J. 2011;30(5):800–13. doi:10.1038/emboj.2011.10.
102. Yu Z, Pestell TG, Lisanti MP, Pestell RG. Cancer stem cells. Int J Biochem Cell Biol. 2012;44(12):2144–51. doi:10.1016/j.biocel.2012.08.022.

103. Li Y, Laterra J. Cancer stem cells: distinct entities or dynamically regulated phenotypes? Cancer Res. 2012;72(3):576–80. doi:10.1158/0008-5472.CAN-11-3070.
104. Levina V, Marrangoni A, Wang T, Parikh S, Su Y, Herberman R, et al. Elimination of human lung cancer stem cells through targeting of the stem cell factor–c-kit autocrine signaling loop. Cancer Res. 2010;70(1):338–46. doi:10.1158/0008-5472.CAN-09-1102.
105. Xiao H, Wang J, Liu Y, Li L. Relative influence of c-Kit expression and epidermal growth factor receptor gene amplification on survival in patients with non-small cell lung cancer. Oncol Lett. 2014;8(2):582–8.
106. Lu H-Y, Zhang G, Cheng Q-Y, Chen B, Cai J-F, Wang X-J, et al. Expression and mutation of the c-kit gene and correlation with prognosis of small cell lung cancer. Oncol Lett. 2012;4(1):89–93.
107. Herpel E, Jensen K, Muley T, Warth A, Schnabel PA, Meister M, et al. The cancer stem cell antigens CD133, BCRP1/ABCG2 and CD117/c-KIT are not associated with prognosis in resected early-stage non-small cell lung cancer. Anticancer Res. 2011;31(12):4491–500.